# Estimating the Accuracy of Coarse Scale Classification Using High Scale Information

**Christiane Klöditz, Angelien van Boxtel, Elisabetta Carfagna, and Willem van Deursen**

## Abstract

*A method is proposed to estimate the classification accuracy of low-resolution images by using high-resolution images in place of ground truth information. For that reason, low-resolution pixels have been simulated by degrading high-resolution images using different multi-resolution techniques. We carried out a statistical analysis, resulting in two models that combine the information from the aggregated high-resolution Landsat TM Normalized Difference Vegetation Index (NDVI) data in order to predict NOAA NDVI data. The method is illustrated by a case study on mapping surface roughness of different landscape classes in order to determine the amount of deposition of atmospheric pollutants.*

## Introduction

At present, the ground resolution of remote sensing images can range from about 5 by 5 m to more than 1 by 1 km. The choice of the appropriate resolution depends on the information desired as well as the spatial structure of the scene itself. Most commonly used are spatial resolutions of 20 to 30 m as available from the SPOT and Landsat Thematic Mapper (TM) satellites, respectively. However, data with a coarser resolution such as from NOAA (1 by 1 km) are being used at the same time. High-resolution images provide a lot of detail information, but at the same time a large amount of data needs to be processed. In comparison, a lower resolution provides sufficient information for many applications, and the amount of data required is much less in quantity.

Moody *et al.* (1994) pointed out the necessity for efforts devoted to the validation and accuracy assessment of lower resolution data sets, which raises the issue of using high-resolution land-cover information from local maps and/or from remotely sensed sources. Loveland *et al.* (1991) stated that there were no adequate existing methods to verify 1-km resolution land-cover classifications conducted over large areas.

This paper addresses the estimation of classification accuracy of remote sensing images at a coarse scale using high-resolution images. Based on ground truth measurements, an evaluation of the classification accuracy of high-resolution Landsat TM images is possible. However, this is not feasible for lower resolution images, such as NOAA images, because of the fact that ground measurements would be laborious and cover in practice only a very small part of the pixels in these images. The method proposed here is to use classified high-resolution images to estimate the accuracy of the classification of low-resolution images. In order to do this, the Landsat TM images have to be degraded to the lower resolution of NOAA images. Once satisfactory degradation results are achieved, the Landsat TM images can be evaluated more easily and can be used as "ground truth" data for low-resolution images. Based on that idea, we performed a study on the degradation of high-resolution Landsat TM images (30 by 30 m) to the resolution of NOAA images (1 by 1 km). The concepts are illustrated by a case study on the mapping of the roughness characteristics of land surfaces. In vegetation, these characteristics are determined by the canopy structure or roughness of the vegetation. The most acidifying air pollutants in Europe — $SO_x$, $NH_x$, and $NO_x$ — are deposited at rates that are affected by these roughness characteristics. Roughness length maps created by processing remote sensing images have been used as inputs to the deposition model DEADM (Erisman, 1992) in order to quantify the deposition of pollutants. This model calculated the total potential acid deposition at scales of 1 by 1 km or 5 by 5 km. Landsat TM images have been used to produce appropriate roughness length maps. However, in order to cover the whole of Europe, maps at different scales are necessary, coarser than 1 by 1 km or 5 by 5 km, using lower resolution images such as NOAA. For that reason, the objective of this study was to find a relation between simulated and originally low-resolution images. The degradation methods presented are based on multi-resolution techniques. A statistical analysis of the pixels in the low-resolution image in comparison with the pixels at the same position in the simulated low-resolution images was carried out. This enabled the development of statistical models for the simulation of low-resolution pixels from high-resolution pixels. It is obvious that these models can only be seen as precise for that certain case. They are restricted, meaning that using other data can result in other models.

The main objective of this paper is to describe the method, illustrated by one example. Tests on other sites are recommended. However, the study shows that it is possible to predict low-resolution data by high-resolution information. Our study was carried out using one Landsat TM NDVI image and one NOAA NDVI image of the same area in The Netherlands. An important step in view of the further processing of images with different resolutions is the geometrical registration of the images.

A method for the automatic registration of images based on a multi-resolution decomposition of the images was pre-

C. Klöditz, A. van Boxtel, and W. van Deursen are with Resource Analysis, Zuiderstraat 110, 2611 SJ Delft, The Netherlands.

E. Carfagna is with the Dipartimento di Scienze Statistiche, via Belle Arti, 41 - 40126 Bologna, Italy.

Photogrammetric Engineering & Remote Sensing, Vol. 64, No. 2, February 1998, pp. 127–133.

0099-1112/98/6402-127$3.00/0

sented in Djamdji *et al.* (1993). The method had been applied to images obtained with identical sensors, as well as with different sensors. They mentioned that the main difficulty for geometric correction lies in finding ground control points (GCP); features located in both the input image and the reference image. That is, because the determination of these points affects the quality of the registration.

For our study, the high-resolution image was geometrically registered to the low-resolution image. After defining a set of ground control points, the geometrical registration of the images was carried out iteratively. The main questions to be answered in this study were: Which are the features in the high-resolution image having the most influence when simulating a low-resolution pixel? How much information will be lost due to a lower resolution? and Can we attain as much information from low-resolution images as from high-resolution images?

## Background

The spatial resolution of an image determines which objects can be recognized. In an image with a ground resolution of 80 by 80 m, a suburban area is seen as a region, while its components (houses, etc.) are subresolution and cannot be seen. A spatial resolution finer than the objects in the scene results in radiance values very similar for neighboring pixels. With increasing resolution, more objects are found in one resolution cell. The role of resolution has been investigated for different applications in several studies.

Woodcock and Strahler (1987) proposed a method to determine the appropriate spatial resolution based on the measuring of the local variance as a function of the spatial structure in images. By simply averaging a number of cells resulting in one single larger cell, the images have been degraded to coarser resolutions. In order to measure local variance at multiple resolutions, the standard deviation of the pixels in a 3 by 3 window was calculated. Each pixel in the image was considered the center of the 3 by 3 window, and the mean of the standard deviation values has been taken as an indication of local variance in the whole image.

Marceau *et al.* (1994a, 1994b) addressed the identification of the optimal spatial resolution for the detection and discrimination of coniferous classes in a forested environment. The most important question was at which scale measurements should be taken in order to provide a representative observation. They showed that, due to the direct link between a particular resolution and real object sizes, the sampling systems can be adapted to the characteristics of the phenomena of interest. The steps of the methodology proposed in the paper included an *a priori* definition of the geographical entities of interest and the aggregation of the data acquired from a fine spatial grid. They pointed out three situations that can occur working with remote sensing images: a pixel size smaller than, equal to, or larger than the geographical entity under investigation. In the first situation, the spatial resolution can be aggregated to the size of these geographical entities. This approach was also based on the degradation of the original data to coarser spatial resolution by averaging neighboring pixels in an odd-sized window (3 by 3, 5 by 5, etc.), resulting in a series of images at different resolutions.

In Cushnie (1987), a study on the effects of spatial resolution on classification accuracy was presented. The study area contained a residential area of high internal variability surrounded by large homogeneous fields of low internal variability. Images with a high resolution (5 by 5 m, 10 by 10 m) were degraded in order to simulate lower resolutions (10 by 10 m, 20 by 20 m). Within the internally homogeneous classes, the classification accuracy was high at all resolutions while for the classes with a high internal variability the classification accuracy improved as spatial resolution was coarsened.

An interesting study on methods for the resolution enhancement of multispectral images using higher resolution panchromatic images is described in Munechika *et al.* (1993). Irons *et al.* (1985) examined the effects of the spatial resolution on the classification of Landsat TM images. In order to simulate the 80-m resolution of the Landsat Multispectral Scanner (MSS), high-resolution Landsat-4 TM data (30-m resolution) were degraded, approximating the impacts of the MSS sensor characteristics by convolution with a 3 by 3 unweighted average filter.

Moreno *et al.* (1992) presented a method that combined high-resolution data (SPOT images) with low-resolution data (NOAA AVHRR images) based on the assumption that each elementary member of a low-resolution NOAA pixel can be considered as a high-resolution SPOT pixel. The method was described as a practical way of estimating inputs to models which require high- as well as low-resolution data inputs. An application on surface temperature mapping was presented. Therefore, a high-resolution emissivity map derived from SPOT data had been combined with NOAA thermal data. The transition of (very high spatial resolution) ground-truth data into high-resolution data, and from these to low-resolution data was pointed out as a practical way of integrating ground-truth data into low-resolution data. This idea was the starting point of the study presented in this paper. The studies mentioned above have in common that all of them consider one image at different resolutions for different purposes. Besides the averaging used in these studies, there are many methods proposed for multi-resolution techniques aggregating high-resolution images to lower resolutions. For a description of multi-resolution techniques, the reader is referred to Tanimoto and Pavlidis (1975) and Rosenfeld (1984).

## Methods

The study area is located in The Netherlands in the provinces of Utrecht and Gelderland, consisting of forest and agricultural as well as urban areas. The high-resolution image was a Landsat TM image from May 1993. For the comparison with a low-resolution image, a NOAA scene from June 1993 was used. Instead of the original pixel values, we used NDVI values, which have been shown to be significantly correlated with vegetation parameters as leaf area index and crown coverage. These values result from the combination of the values in different spectral bands of the NOAA and the Landsat TM images, respectively. To simplify the processing, the NDVI values of the images have been rescaled to values between 0 and 255. High NDVI values are associated with great density and greenness of the vegetation, and low values are related to bare soil and urban areas. One disadvantage of NDVI data is that some land-cover types cannot be correctly identified. Through the absence of photosynthetically active plant material, water bodies, snow and ice, and barren land have similar NDVI characteristics (Loveland *et al.*, 1991).

For the construction of the multi-resolution presentation, the computation of the different resolutions was performed in steps by combining a certain number of neighboring pixels using basic operations such as (weighted) averaging and searching for the minimum or the maximum. The Landsat TM pixel block was processed over a 33 by 33 neighborhood to obtain the lower resolution as illustrated in Figure 1a.

Out of the numerous conceivable pyramid techniques, the following were used for the study:

- *Average Pyramid.* The "classical" method to construct a pyramid is the averaging of a non-overlapping 2 by 2 or 3 by 3 pixel block and storing the result of this process in a cell at the next higher level. This process was modified to determine the average of a 33- by 33-pixel block.

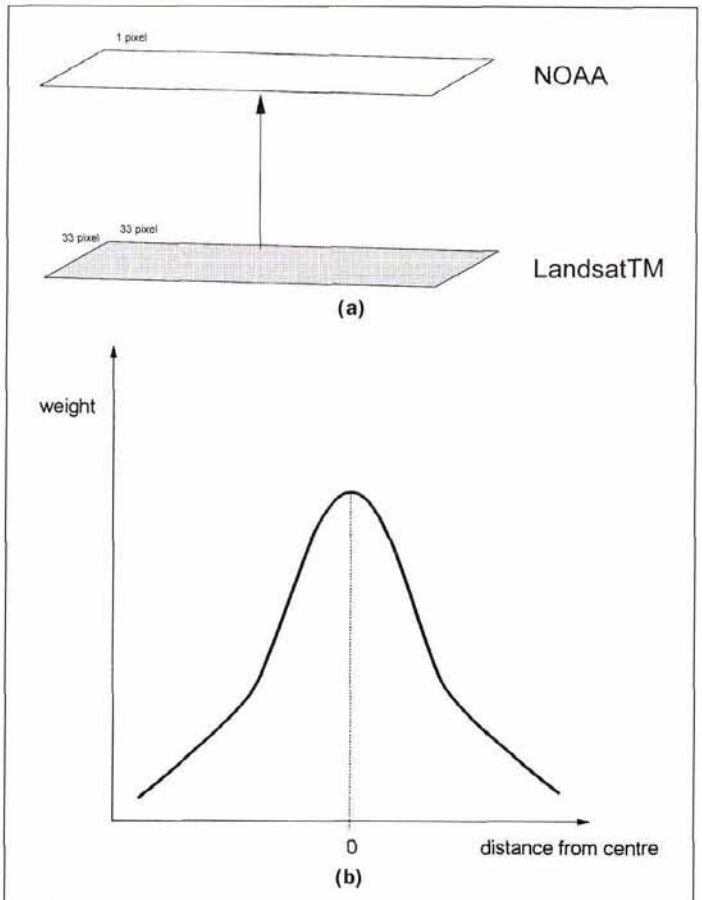


Figure 1. (a) Aggregation process. (b) Gaussian spot - aggregation by weighted averaging.

- *Gauss Pyramid.* This technique was based on the weighted averaging of the pixel block where the weights show a peak in the center of the averaged region and fall off to zero at the border similar to a Gaussian spot as illustrated in Figure 1b.
- *Minimum and Maximum Pyramid.* The minimum or the maximum of the values in the pixel block were taken as the value for the pixel on the next level.
- *Standard Deviation Pyramid.* The standard deviation of the pixels in the pixel block was calculated and used as the value on the next level. The standard deviation can be seen as a measure of the local variability in the image and was therefore an important characteristic for the statistical analysis.

Assuming that every high-resolution pixel within a defined area contributes to the corresponding low-resolution pixel, the loss of information at lower resolution should be rather minimal considering the classification of areas of approximately 1 by 1 km or bigger.

As can be seen in Figures 2a through 2d, the main patterns are preserved in the simulated lower resolution images selected. For a better comparison, the legends of these figures have been brought in line. Figure 2e illustrates the aggregation by using the standard deviation of the pixels in the pixel block.

The most important advantage of the method used, when comparing it with resampling procedures available in GIS, is the possibility of controlling the resampling process and therefore permitting the adaption of the algorithm to the characteristics of the image. Because the goal is not to preserve detailed images but to localize pattern at a scale of 1 by 1 km, the application of the multi-resolution techniques to high-resolution images yields promising results.

## Results

A statistical analysis had been undertaken based on 188 pixels extracted from the resulting pyramid images and the NOAA image. These pixels were selected systematically by overlaying the NOAA image as well as the degraded Landsat TM images with a virtual regular grid and sampling the pixels at the intersection points of the grid.

### Simple Linear Regression

Because we were interested in the relationship of two variables, namely, each pyramid variable and the NOAA variable, a simple linear regression was performed with NOAA as the dependent variable and each of the pyramids as the independent variable. The first analysis was descriptive and was devoted to understanding the behavior of the different kinds of aggregation methods and compare them with NOAA data. Table 1 contains the values of the main statistical parameters: mean, standard deviation, standard error, minimum, and maximum.

Apparently, the parameters of the average pyramid were the most similar to the NOAA ones, although the distribution of the average values was a little shifted and more concentrated observing the minimum and maximum values. Maximum and minimum pyramids had quite different parameters from the NOAA parameters. Because the standard deviation is a measure of dispersion, the significant difference between standard deviation pyramid values and NOAA values is obvious. The reason why it was taken into account was that it could help another degradation method to predict NOAA data in a multivariate analysis. It gave information about the dispersion of NDVI values of TM pixels corresponding to each NOAA pixel. The correlation matrix of the different pyramid images seen in Table 2 was very useful to get an idea of what kind of model could be built.

The correlation index varied between $-1$ and $+1$ and expressed the level of linear link between two variables. All degraded images had a positive correlation with NOAA. For most of the images, the correlation was so low (values near zero) that a hypothesis of a linear link between NOAA and those images was not reliable. However, the linear correlation coefficient for NOAA and the average image was relevant ($R = 0.540$) and the test for significance of the difference of the correlation from zero gave a very low error probability ($p < 0.0001$). Thus, the average was useful to try to explain the behavior of NOAA data. The linear determination index (R squared) seen in Table 3 was not high enough to presume a linear link between NOAA and the pyramid images.

However, the linear determination index for the average values (0.292) is not significant but higher than the others and indicates that approximately 30 percent of the variance of the NOAA variable can be explained by the average variable. Figure 3 shows the graph of the average values versus NOAA values.

For the other pyramid variables, these percentages were very low, meaning that they cannot be used alone to predict the NOAA values. Therefore, the model we attempted was based on multiple regression.

### Multiple Linear Regression

With the help of multiple linear regression, we analyzed the link between some of the above-mentioned pyramid variables and NOAA. The correlation matrix (Table 2) shows that some of the pyramid variables were loosely correlated with NOAA. That is why we did not select them to explain the NOAA variable in a simple regression model. On the other hand, some degradation methods showed a noticeable correlation between them, as for instance between the Gauss and the maximum method (0.555), between the maximum and the standard deviation method (0.523), between the Gauss and the

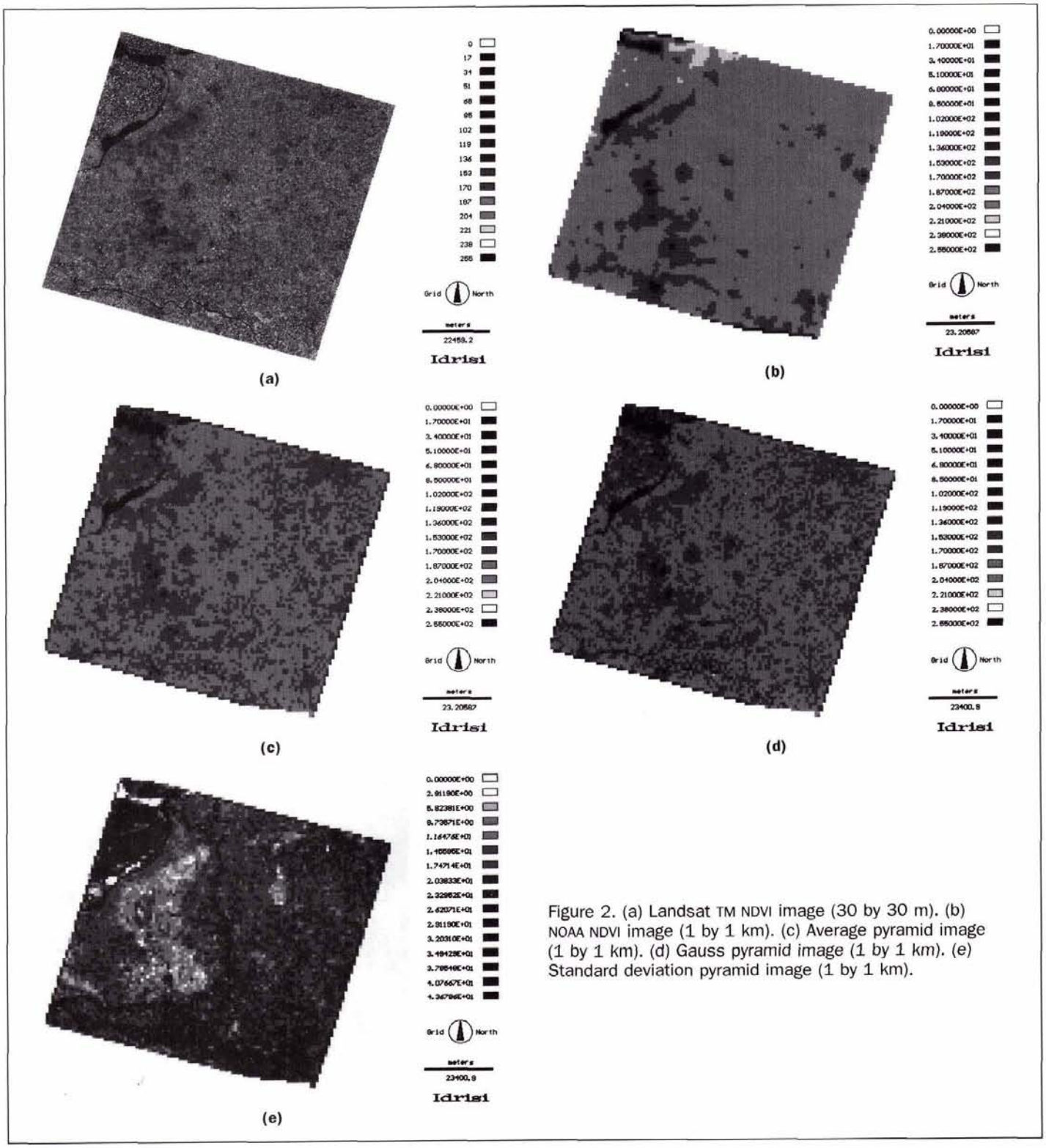


Figure 2. (a) Landsat TM NDVI image (30 by 30 m). (b) NOAA NDVI image (1 by 1 km). (c) Average pyramid image (1 by 1 km). (d) Gauss pyramid image (1 by 1 km). (e) Standard deviation pyramid image (1 by 1 km).

minimum method (0.462), and between the minimum and the standard deviation method (−0.489). Although the correlation was not high, including two correlated variables in a model could result in a redundancy of information and instability of the model. Therefore, low correlated variables had to be chosen. To select the best subset of available pyramid variables, we adapted a stepwise regression. This method tests if the increment of explained variance of the dependent variable due to the introduction of a new variable in the model is relevant, with a probability level that can be selected. The same criterion was used to eliminate variables from the model after the inclusion of others. Various combinations of variables have been tested. The selection procedure individuated the combination that explained the highest amount of variance of the dependent variable (NOAA NDVI). Different probability levels have been tried, starting with low probability levels of making an error in the test. That is to say that the inclusion of a variable in the model was ac-

TABLE 1. DESCRIPTIVE STATISTICS

| | NOAA | Maximum pyramid | Minimum pyramid | Standard-deviation pyramid | Average pyramid | Gauss pyramid |
|---|---|---|---|---|---|---|
| Mean | 183.686 | 206.774 | 130.362 | 17.578 | 172.455 | 173.198 |
| Std.Dev | 16.166 | 8.083 | 16.115 | 6.303 | 15.509 | 14.766 |
| Std.Error | 1.179 | 0.590 | 1.175 | 0.460 | 1.131 | 1.077 |
| Minimum | 97.000 | 170.351 | 0.786 | 3.928 | 96.265 | 104.935 |
| Maximum | 208.000 | 214.772 | 165.906 | 38.661 | 199.642 | 196.674 |

TABLE 2. CORRELATION MATRIX (R)

| | NOAA | Maximum | Minimum | Standard-deviation | Average | Gauss |
|---|---|---|---|---|---|---|
| NOAA | 1.000 | | | | | |
| Maximum | 0.162 | 1.000 | | | | |
| Minimum | 0.031 | 0.069 | 1.000 | | | |
| Std.Dev. | 0.086 | 0.523 | −0.489 | 1.000 | | |
| Average | 0.540 | 0.172 | 0.051 | −0.140 | 1.000 | |
| Gauss | 0.028 | 0.555 | 0.462 | −0.140 | 0.157 | 1.000 |

TABLE 3. LINEAR REGRESSION WITH NOAA AS DEPENDENT VARIABLE

| | linear determination index (R squared) |
|---|---|
| NOAA vs. Average | 0.292 |
| NOAA vs. Gauss | 0.001 |
| NOAA vs. Minimum | 0.001 |
| NOAA vs. Maximum | 0.026 |
| NOAA vs. Standard deviation | 0.007 |
| NOAA vs. 5 independents | 0.337 |
| NOAA vs. 2 independents (Model 1) | 0.319 |
| NOAA vs. 3 independents (Model 2) | 0.328 |

cepted only if its contribution was relevant. On the other hand, the elimination of one variable was only done if the evidence of its importance in the model was not very big. The result was a model with the independent variables average and standard deviation, which was

$$\text{Model 1: NOAA} = A + B * \text{average} + C * \text{standard deviation},$$

with, in our particular case, $A = 74.968$, $B = 0.587$, and $C = 0.424$.

Using a higher probability level, another independent variable, the minimum, was included and the model was

$$\text{Model 2: NOAA} = D + E * \text{average} + F * \text{standard deviation} + G * \text{minimum},$$

with $D = 57.86$, $E = 0.589$, $F = 0.562$, and $G = 0.11$ in our study.

Analyzing this model, the regression coefficient of the minimum variable was very low (0.11), meaning that the influence of the minimum was not significant. Besides, the correlation between the minimum and the standard deviation variable was rather high. This can cause instability of the model. The percentage of variance of the dependent variable explained by both models was similar, 32.8 percent for Model 2 and 31.9 percent for Model 1. See Table 3 for the linear determination index for both models as well as the first test with all five pyramid variables.

The value for Model 1 was not much lower than that for Model 2, but it was more robust. It showed 85 negative and 103 positive residuals (errors). The values and the pattern of the residuals were very important. They are the difference between the dependent variable values and the ones predicted by the models. Most of them were in the range of −20 to 20. Some very high absolute values of the residuals — the highest was (−)52 — indicated that there were some NOAA values that the model was not able to predict. This was the case for both models. Some residuals were very small, ranging from −1 to 1. These values gave an idea of the possible errors that can occur using estimates instead of NOAA data. For about 150 NOAA pixels, the NDVI value can be estimated with a relative residual in the range of −10 to 10. In the graph with residuals versus NOAA NDVI in Figure 4, it is evident that the models were not able to predict very low NOAA values. In fact, NOAA values from about 98 to 140 were considerably overestimated. Furthermore, the models tended to overestimate less significantly NOAA data from about 140 to 170 and to underestimate data from 195 to 210. In the range of 170 to 195, the data were predicted very well. Because about 60 percent of the NOAA values in our study occurred in this range, the simulation of low resolution data was promising with both models. NDVI values in this range belong to forest land-cover types.

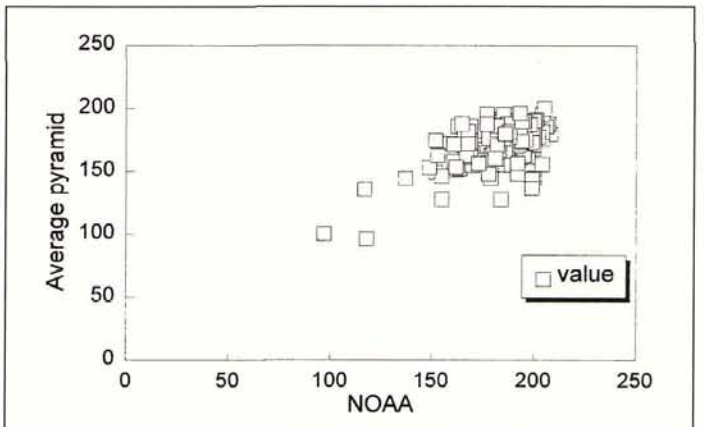

Figure 3. Average pyramid vs. NOAA.

The values simulated with the models versus the original NOAA values are illustrated in Figures 5 and 6, respectively.

## Conclusions and Recommendations

The method used in the study was based on the use of a set of high-resolution data (Landsat TM) in order to predict low-resolution data (NOAA). Naturally, the high-resolution Landsat TM image contained more information than did the NOAA image. However, the lower resolution of NOAA is more appropriate for roughness length mapping on a large scale.

Two models were found in this experiment, both approximating NOAA NDVI values. The values simulated by the models are similar. Both models tended to predict NOAA NDVI values in the range of 195 to 210 very well, which was the range where 60 percent of the values occurred. The study showed that the use of Landsat TM data as a substitute for required ground truth information is a possible way to estimate the accuracy of coarse scale classification. If these models are shown to be valid, they can be used to determine the influence of high-resolution elements within low-resolution pixels. Both models consider the average over the 33- by 33-pixel block and the standard deviation as having the most influence when simulating the low-resolution NOAA pixel. The standard deviation expresses the local variability in the pixel block and the average represents the occurance of a certain vegetation pattern. Therefore, it was concluded that this method is applicable in regions with local variability and vegetation patterns similar to those of the study area. Be-

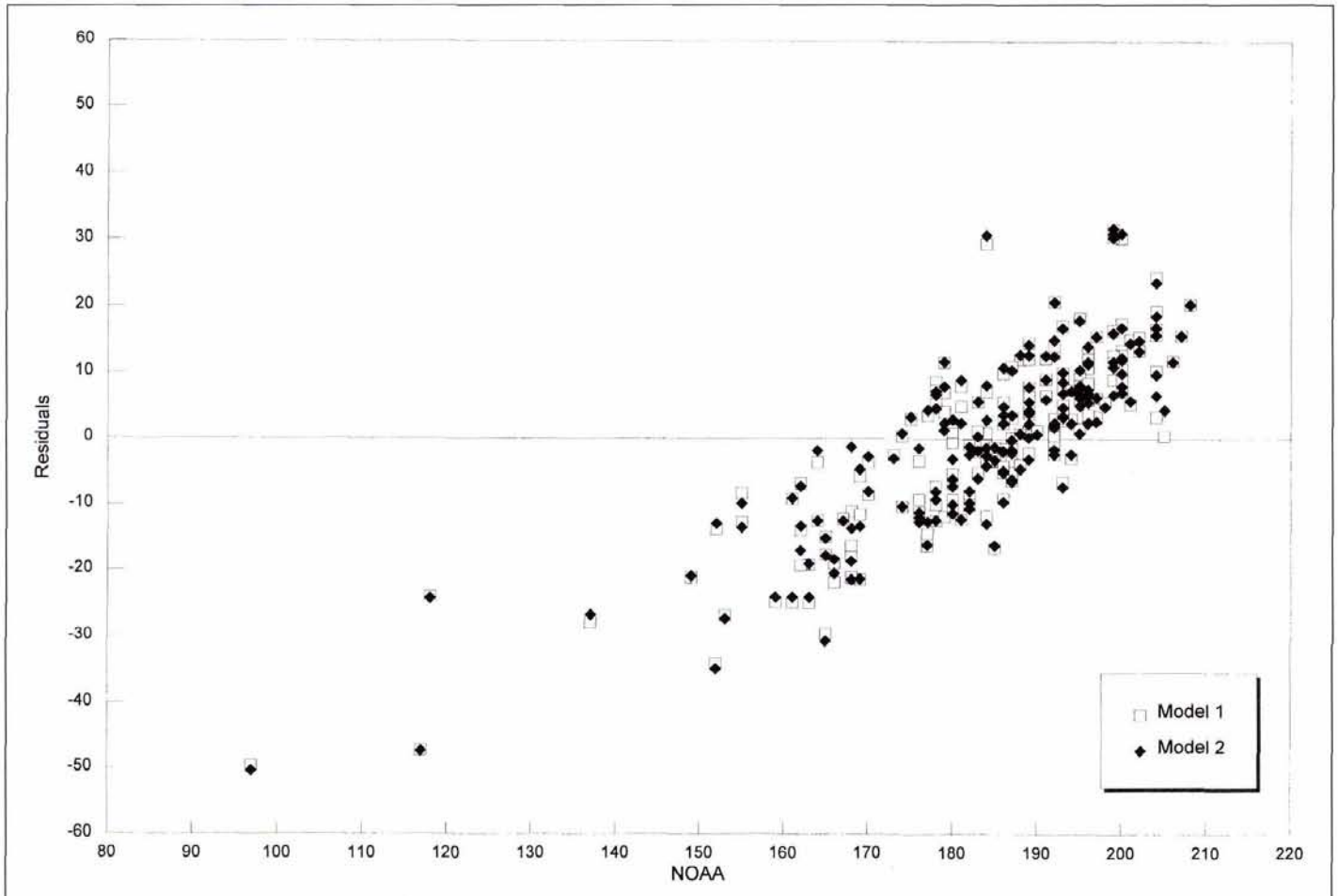


Figure 4. Residuals of Model 1 and Model 2 vs. NOAA.

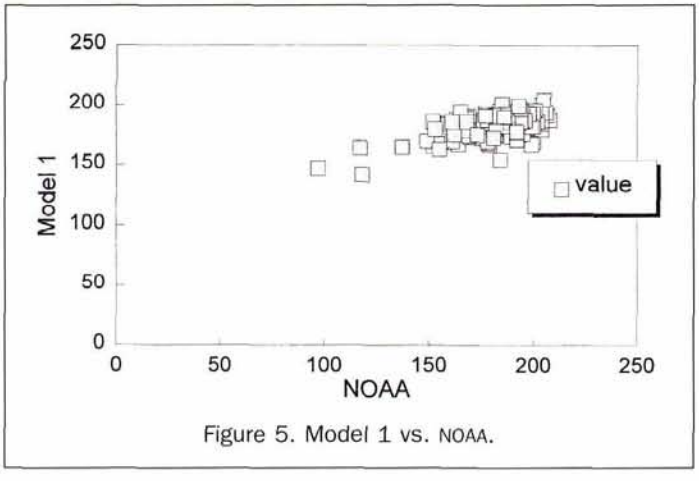


Figure 5. Model 1 vs. NOAA.

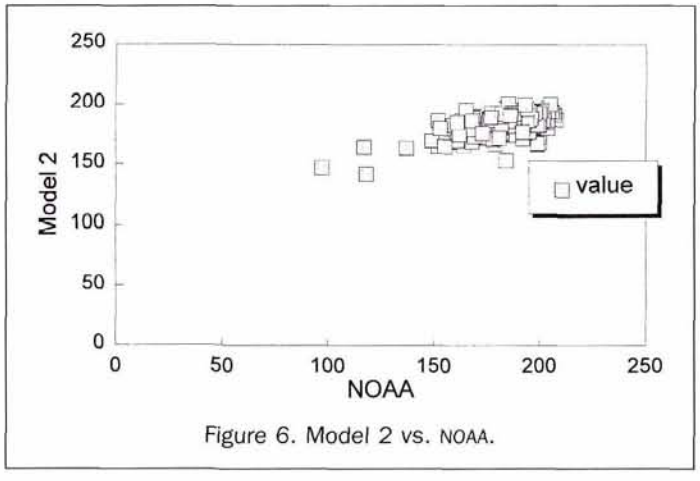


Figure 6. Model 2 vs. NOAA.

cause other areas in Europe show this similarity, it is assumed that comparable results can be achieved. The overall objective of this paper was to illustrate the suitability of high-resolution data to predict low-resolution information in a single experiment. For that objective, the experiment was successful.

Further research on this subject is highly recommended. It should include tests of the applicability of the method in regions where no Landsat TM images are available. Another aspect of future work should be the search for a nonlinear model that might result in even better simulation values. The applicability of the methodology has yet to be proven for images other than NDVI images.

## References

Cushnie, J.L., 1987. The interactive effect of spatial resolution and degree of internal variability within land-cover types on classification accuracies, *Int. J. Remote Sensing*, 8(1):15–29.

Djamdji, J.-P., A. Bijaoui, and R. Maniere, 1993. Geometrical registra-

tion of images: The multiresolution approach, *Photogrammetric Engineering & Remote Sensing*, 59(5):645–653.

Erisman, J.W., 1992. *Atmospheric Deposition of Acidifying Compounds in The Netherlands*, Ph.D. Dissertation, Rijksuniversiteit Utrecht, Utrecht, The Netherlands.

Irons, J.R., R.S. Latty, B.L. Markham, R.F. Nelson, M.L. Stauffer, D.L. Toll, and D.L. Williams, 1985. The effects of spatial resolution on the classification of Thematic Mapper data, *Int. J. Remote Sensing*, 6(8):1385–1403.

Loveland, T.R., J.W. Merchant, D.O. Ohlene, and J.F. Brown, 1991. Development of a land-cover characteristics database for the conterminous U.S., *Photogrammetric Engineering & Remote Sensing*, 57(11):1453–1463.

Marceau, J.D., D.J. Gratton, and P.J. Howarth, 1994a. Remote sensing and the measurement of geographical entities in a forested environment. 1. The scale and spatial aggregation problem, *Remote Sensing Environ.*, 49:93–104.

Marceau, J.D., R.A. Fornier, J.-P. Fortin, and D.J. Gratton, 1994b. Remote sensing and the measurement of geographical entities in a forested environment. 2. The optimal spatial resolution, *Remote Sensing Environ.*, 49:105–117.

Moody, A., and C.E. Woodcock, 1994. Scale-dependent errors in the estimation of land-cover proportions: Implications for global land-cover datasets, *Photogrammetric Engineering & Remote Sensing*, 60(5):585–594.

Moreno, J.F., J. Melia, and G. Soledad, 1992. Geometric integration of NOAA AVHRR and Spot Data: Low resolution effective parameters from high resolution data, *IEEE Transactions on Geoscience and Remote Sensing*, 30(5):1006–1014.

Munechika, C.K., J.S. Warnick, C. Salvaggio, and J.R. Schott, 1993. Resolution enhancement of multispectral image data to improve classification accuracy, *Photogrammetric Engineering & Remote Sensing*, 59(1):67–72.

Rosenfeld, A., 1984. *Multiresolution Image Processing and Analysis*, Springer-Verlag, Berlin.

Tanimoto, S.L., and T. Pavlidis, 1975. A hierarchical data structure for picture processing, *Computer Graphics and Image Processing*, 4(2):104–119.

Woodcock, C.E., and A.H. Strahler, 1987. The factor of scale in remote sensing, *Remote Sensing Environ.*, 21:311–332.

Received 10 June 1995; revised & accepted 14 April 1997; revised 18 June 1997)

## ➤ ➤ FORTHCOMING ARTICLES ➤ ➤ ➤ ➤ ➤

*Michel Arnaud* and *Albert Flori*, Bias and Precision of Different Sampling Methods for GPS Positions.

*Stéphane Chalifoux, François Cavayas*, and *James T. Gray*, Map-Guided Approach for the Automatic Detection on Landsat TM Images of Forest Stands Damaged by the Spruce Budworm.

*Warren B. Cohen, Maria Fiorella, John Gray*, and *Karen Anderson*, An Efficient and Accurate Method for Mapping Forest Clearcuts in the Pacific Northwest Using Landsat Imagery.

*F. Deppe*, Forest Area Estimation Using Sample Surveys and Landsat MSS and TM Data.

*Sheldon D. Drobot* and *David G. Barber*, Towards Development of a Snow Water Equivalence (SWE) Algorithm Using Microwave Radiometry over Snow Covered First-Year Sea Ice.

*Hamid Ebadi* and *Michael A. Chapman*, GPS Controlled Strip Triangulation Using Geometric Constraints of Man-Made Structures.

*Jay Gao* and *Matthew B. Lythe*, Effectiveness of the MCC Method in Detecting Oceanic Circulation Patterns at a Local Scale from Sequential AVHRR Images.

*J.R. Harris, A.N. Rencz, B. Ballantyne*, and *C. Sheridon*, Mapping Altered Rocks Using Landsat TM and Lithogeochemical Data: Sulphurets-Brucejack Lake District, British Columbia, Canada.

*Stanley R. Herwitz, Robert E. Slye*, and *Stephen M. Turton*, Co-Registered Aerial Stereopairs from Low-Flying Aircraft for the Analysis of Long-Term Tropical Rainforest Canopy Dynamics.

*Fabio Maselli, Ljiljana Petkov*, and *Giampiero Maracchi*, Extension of Climate Parameters Over the Land Surface by the Use of NOAA-AVHRR and Ancillary Data.

*Robb D. Macleod* and *Russell G. Congalton*, A quantitative Comparison of Change Detection Algorithms for Monitoring Eelgrass from Remotely Sensed Data.

*Kenneth C. McGwire*, Mosaicking Airborne Scanner Data with the Multiquadric Rectification Technique.

*Kenneth C. McGwire*, Improving Landsat Scene Selection Systems.

*Victor Mesev*, The Use of Census Data in Urban Image Classification.

*Jeffrey T. Morisette* and *Siamak Khorram*, Exact Binomial Confidence Interval for Proportions.

*S.V. Muller, S.A. Walker, F.E. Nelson, N.A. Auerbach, J.G. Bockheim, S. Guyer*, and *D. Sherba*, Accuracy Assessment of a Land-Cover Map of the Kuparuk River Basin Alaska: Considerations for Remote Sensing.

*Ram M. Narayanan* and *Brian D. Guenther*, Effects of Emergent Grass on Mid-Infrared Laser Reflectance of Soil.

*Elijah W. Ramsey III, Dal K. Chappell, Dennis Jacobs, Sijan K. Sapkota*, and *Dan G. Baldwin*, Resource Management of Forested Wetlands: Hurricane Impact and Recovery Mapped by Combining Landsat TM and NOAA AVHRR Data.

*Juliang Shao* and *Clive S. Fraser*, Scale-Space Methods for Image Feature Modeling in Vision Metrology.

*K.M.S. Sharma* and *A. Sarkar*, A Modified Contextual Classification Technique for Remote Sensing Data.

*Yongwei Sheng, Yafang Su*, and *Qianguang Xiao*, Challenging the Cloud-Contamination Problem in Flood Monitoring with NOAA/AAVHRR Imagery.

*Andrew K. Skidmore*, Nonparametric Classifier for GIS Data Appliedto Kangaroo Distribution Mapping.

*E. Terrence Slonecker, Denice M. Shaw*, and *Thomas M. Lillesand*, Emerging Legal and Ethical Issues in Advanced Remote Sensing Technology.

*Randolph H. Wynne, Thomas M. Lillesand, Murray K. Clayton*, and *John J. Magnuson*, Satellite Monitoring of Lake Ice Breakup on the Laurentian Shield (1980-1994).

*David A. Yocky* and *Benjamin F. Johnson*, Repeat-Pass Dual-Antenna Synthetic Aperture Radar Interferometric Change Detection Post-Processing.